Repeated and Controlled Growth of Monolayer, Bilayer and Few-Layer Hexagonal Boron Nitride on Pt Foils

Yang Gao,[†] Wencai Ren,[†,*] Teng Ma,[†] Zhibo Liu,[†] Yu Zhang,[‡] Wen-Bin Liu,[†] Lai-Peng Ma,[†] Xiuliang Ma,[†] and Hui-Ming Cheng[†,*]

[†]Shenyang National Laboratory for Materials Science, Institute of Metal Research, Chinese Academy of Sciences, 72 Wenhua Road, Shenyang 110016, People's Republic of China, and [‡]State Key Laboratory of Robotics, Shenyang Institute of Automation, Chinese Academy of Sciences, 114 Nanta Street, Shenyang 110016, People's Republic of China

ABSTRACT Atomically thin hexagonal boron nitride (h-BN), as a graphene analogue, has attracted increasing interest because of many fascinating properties and a wide range of potential applications. However, it still remains a great challenge to synthesize high-quality h-BN with predetermined number of layers at a low cost. Here we reported the controlled growth of h-BN on polycrystalline Pt foils by low-cost ambient pressure chemical vapor deposition with ammonia borane as the precursor. Monolayer, bilayer and few-layer h-BN domains and large-area films were selectively obtained on Pt by simply changing the concentration of ammonia borane. Moreover, using a bubbling method, we have achieved the nondestructive transfer of h-BN from Pt to arbitrary substrates and the repeated use of the Pt for h-BN growth, which not only reduces environmental pollution but also decreases the production cost of h-BN. The monolayer and bilayer h-BN obtained are very uniform with high quality and smooth surfaces. In addition, we found that the optical band gap of h-BN increases with decreasing number of layers. The repeated growth of large-area, high-quality monolayer and bilayer h-BN films, together with the successful growth of graphene, opens up the possibility for creating various functional heterostructures for large-scale fabrication and integration of novel electronics.

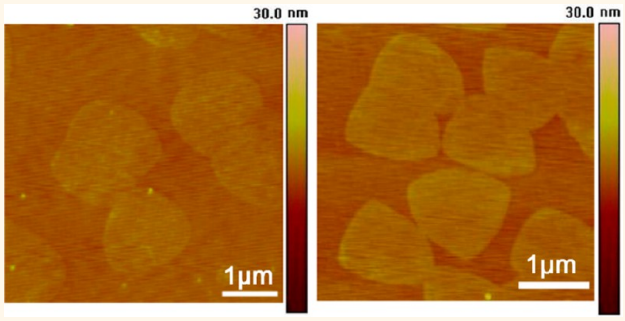

KEYWORDS: hexagonal boron nitride · monolayer · bilayer · chemical vapor deposition · bubbling transfer

Since the isolation of graphene from graphite in 2004, graphene and other two-dimensional (2D) atomic crystals have attracted increasing interest because of their unique structure, many fascinating properties and a wide range of technological applications.[1−3] Atomically thin hexagonal boron nitride (h-BN), as a graphene analogue, is a wide band gap insulator with a lattice constant similar to graphene, and has very high mechanical strength and good thermal conductivity because of the strong B−N covalent sp^2 bonds in the plane, as well as excellent chemical and thermal stability.[4−8] As a result, h-BN has a wide range of applications, such as deep ultraviolet light emitters, transparent membranes, protective coatings, and dielectric layers.[4,5,9] In addition, h-BN layers have great potential for use as a constituting layer combined with graphene in creating a new class of functional multilayer heterostructures and devices.[10−14] Previous studies have shown that h-BN can be used as a substrate to improve the electron mobility in graphene for graphene electronics because of its atomically smooth surface that is relatively free of dangling bonds and trapped charges.[11,12] Recently, h-BN has been used as a barrier layer between two graphene layers to construct vertical tunneling transistors.[13,14] Similar to graphene, controlled synthesis of large-area high-quality h-BN with different numbers of layers is essential for both fundamental studies and technological applications. For example, Britnell *et al.* have demonstrated that the tunnel current in a tunnel diode with h-BN as a barrier layer decreases exponentially with the number of h-BN layers.[14]

* Address correspondence to wcren@imr.ac.cn, cheng@imr.ac.cn.

Received for review February 23, 2013 and accepted May 10, 2013.

Published online May 10, 2013
10.1021/nn4009356

Currently, several methods have been developed to prepare atomically thin h-BN including micromechanical cleavage,[13−17] liquid-phase exfoliation,[18] and chemical vapor deposition (CVD).[7,12,19−27] Among them, CVD has shown great potential to prepare large-area h-BN films, which opens up possibilities for the use of h-BN in large-scale electronics. Large-area inhomogeneous few-layer and multilayer h-BN films have been prepared on polycrystalline Cu or Ni by using low-cost ambient pressure CVD (APCVD) with ammonia borane (H_3BNH_3, also called borazane) or borazine as precursors.[7,12,19] Monolayer h-BN was first synthesized in ultrahigh vacuum (UHV) systems mostly using borazine as a precursor and single-crystal metals such as Pt(111), Rh(111), Ru(0001), Cu(111) and Ni(111) as substrates.[20−23,25,26] Recently, Kim *et al.* realized the growth of monolayer h-BN on Cu foil by using low-pressure CVD (LPCVD) with borazane as the precursor.[24] Ismach *et al.* showed controlled synthesis of h-BN with number of layers from 1−5 to ∼100 on Ni foil using LPCVD with diborane and ammonia as precursors.[27] However, it is still very challenging to precisely control the number of layers of h-BN by CVD. In addition, the metal substrates were usually etched away after h-BN growth by a suitable etchant in order to transfer the h-BN to other substrates for further studies and applications.[7,12,19,24,27] This substrate-etching transfer method not only produces serious environmental pollution, but also increases the production cost of h-BN. Moreover, these processes are not suitable for the transfer of h-BN from chemically inert, noble metal substrates, because they are either difficult to etch away completely or have a high cost.

Here we report the controlled growth of monolayer, bilayer and few-layer h-BN domains and large-area continuous films on polycrystalline Pt foils by APCVD with borazane as the precursor. Compared to UHV growth and LPCVD, APCVD growth avoids the use of specific reaction systems and is much easier, which should be very useful for the large-scale production of h-BN at a low cost. Moreover, using an electrochemical bubbling method, which has been recently developed for the nondestructive transfer of graphene,[28] we have achieved the nondestructive transfer of h-BN from Pt to arbitrary substrates and the repeated use of Pt for h-BN growth, which not only reduces pollution but also further decreases the production cost. Importantly, the monolayer and bilayer h-BN obtained are very uniform with high quality and a smooth surface. The synthesis of such h-BN allows for studies on the effect of the number of layers on their different properties. As an example, we found that the optical band gap of h-BN increases with decreasing number of layers.

Borazane is a crystalline solid at room temperature and melts at around 106 °C. For CVD growth of h-BN, the borazane powder was first heated to a temperature (T_1) of 70−80 °C to generate borazane vapor that was then carried into the high-temperature reaction zone (T_2) of 1000 °C by gas flow to decompose on Pt foils to form h-BN layers (Figure S1). Here, we controlled the number of layers of h-BN by simply changing the heating temperature of borazane, *i.e.*, the concentration of borazane in the CVD reaction system (Table S1). A longer reaction time was required to form continuous films than isolated domains (Table S1). After CVD growth, similar to the method for the bubbling transfer of graphene,[28] the Pt substrate with the h-BN grown on it was first spin-coated with a thin layer of polymethyl methacrylate (PMMA), and then used as the cathode of an electrolysis cell in a NaOH aqueous solution. After applying a voltage, the PMMA/h-BN layer was detached from the Pt substrate driven by a large number of H_2 bubbles generated by water electrolysis. Finally, the floating PMMA/h-BN layer was collected on target substrates such as SiO_2/Si, quartz and transmission electron microscopy (TEM) grids followed by the removal of the PMMA layer by hot acetone.

RESULTS AND DISCUSSION

Figure 1a,b shows optical images of h-BN domains transferred onto SiO_2/Si substrates (the thickness of

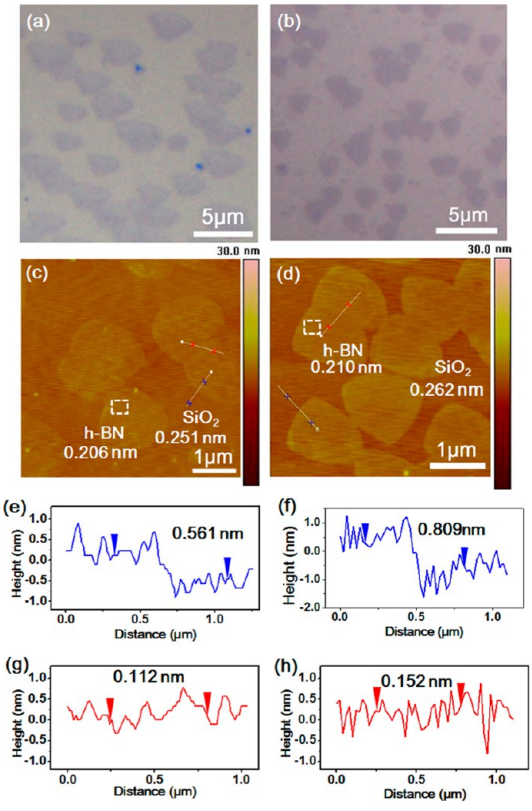

Figure 1. (a and b) Optical and (c and d) AFM images of (a and c) monolayer and (b and d) bilayer h-BN domains transferred onto a SiO_2/Si substrate. The numbers in (c) and (d) show the surface roughness of h-BN domains and SiO_2 substrates. (e and f) The height profiles across a domain in (c) and (d), respectively. (g and h) The height profiles across the joint region of two adjacent domains in (c) and (d), respectively.

the SiO_2 layer is 80 nm), which were prepared at 1000 °C for 50 min with T_1 = 70 and 75 °C. Due to its insulating nature, the h-BN is almost transparent and has a very small contrast with the substrate.[7,17,19,24] Here, the contrast of all optical images was enhanced by a factor of 1.4. It can be seen that all the h-BN domains are triangular with curved edges, which is different from the perfect triangular shape of the h-BN domains grown on Cu foil and Ni(111),[23,24,29] possibly due to the larger lattice mismatch between h-BN and Pt.[30] Moreover, these domains are randomly oriented in the same Pt grain, and the Pt orientation does not show an obvious influence on the shape and density of the h-BN domains (Figure 1d and S2), indicating a weak interaction at h-BN/Pt interface.[30] Such a weak interface interaction allows for the nondestructive separation of h-BN layers from the Pt substrates by the electrochemical bubbling method.

More importantly, the h-BN domains prepared with T_1 = 75 °C show a higher contrast than those prepared with T_1 = 70 °C, indicating a larger thickness. We further characterized these domains using atomic force microscopy (AFM). It is interesting to find that all the h-BN domains prepared with T_1 = 70 °C have a thickness of ~0.561 nm (Figure 1c,e), consistent with a monolayer thickness (*c*-axis spacing for h-BN is ~0.32 nm).[24] In contrast, the typical thickness of the h-BN domains prepared with T_1 = 75 °C is ~0.809 nm (Figure 1d,f), corresponding to a bilayer. Different from the reported CVD grown bilayer graphene domains,[28,31] where the adlayer is usually smaller than the monolayer, the two layers of bilayer h-BN have the same shape and size. Moreover, for the same reaction time, the density of monolayer h-BN domains is smaller than that of bilayer ones, and the monolayer h-BN domains (~2 μm) are larger than the bilayer ones (~1 μm). At T_1 = 80 °C, much smaller few-layer h-BN domains were formed. However, no h-BN was formed at T_1 = 65 °C. These results suggest that we can easily tune the number of layers, nucleation density and the size of h-BN domains on Pt by simply changing the heating temperature of the borazane. This is one of the advantages of APCVD on Pt foils over other methods for h-BN growth, where only inhomogeneous few- and multilayer h-BN films have been prepared on polycrystalline Cu or Ni substrates by APCVD,[7,12,19] and monolayer on Cu foils by LPCVD and on single-crystal metals under UHV conditions.[20−26] Recently, Guo *et al.* demonstrated the control on the size of triangular h-BN domains on the Cu(100) plane by an improved LPCVD, but the samples are lack of control on the number of layers.[29]

The AFM measurements also indicate that the h-BN domains grown on Pt have a very high quality. First, the h-BN domains are intact without cracks or ruptures, indicating that the bubbling transfer method is nondestructive to h-BN because of the weak h-BN/Pt interface interaction mentioned above. Second, almost no wrinkles are found in the monolayer and bilayer h-BN domains. In contrast, the h-BN films and even very small h-BN domains (~1 μm) grown on Cu and Ni show a high density of wrinkles.[7,19,24] The absence of wrinkles is probably due to the smaller difference in thermal expansion coefficients and the weak interaction between Pt and h-BN, and should be beneficial to the use of h-BN in electronics. Third, the h-BN domains are very clean without visible nanoparticles on them, which are usually observed in the h-BN transferred from Cu foils by etching.[7,12,24] Fourth, the h-BN domains are very smooth. The surface roughness of the monolayer and bilayer h-BN domains is about 0.05 nm smoother than that of the SiO_2 substrates on which the h-BN domains are sitting (Figure 1c,d). In addition, it is worth noting that adjacent joining monolayer and bilayer domains are seamlessly connected and the joining regions show a surface roughness similar to that within the domains (Figure 1g,h), which opens up the possibility for preparing continuous and smooth h-BN films.

When increasing the growth time from 50 to 80 min, the monolayer, bilayer and few-layer h-BN domains expand, join, and eventually form continuous films fully covering the Pt substrates, indicating a surface-mediated growth mechanism of h-BN on Pt. Considering the size of the isolated domains shown above, we suggest that the monolayer and bilayer h-BN films are composed of domains larger than ~2 and 1 μm, respectively. Figure 2a−d shows low- and high-magnification optical images of the transferred monolayer and bilayer h-BN films (3 × 1 cm^2) on SiO_2/Si with 80 nm-thick SiO_2. The high transparency of monolayer and bilayer h-BN makes them almost invisible under low-magnification (Figure 2a,b). It is important to note from the high-magnification optical images that the monolayer and bilayer h-BN films are very uniform with very few small additional layers (dark spots, Figure 2c, d). By analyzing many optical images, we found that the area coverage of the additional layers on the monolayer and bilayer h-BN films is 0.12% and 0.19%, respectively (Table S2). AFM measurements confirm that these films prepared at T_1 = 70 and 75 °C are monolayer (~0.566 nm) and bilayer (~0.893 nm) as shown in Figure 2e,f, and this is consistent with the high-resolution TEM observations (Figure 2g,h). Moreover, no more additional layers are formed on monolayer films with increased growth time, and only a very few more additional layers are formed on bilayer h-BN. This is similar to the growth of monolayer h-BN on single-crystal metals under UHV conditions,[21−23,25,26] and different from that on Cu foils by LPCVD,[24] where the number of multilayer regions on monolayer h-BN films remarkably increases with growth time. In addition, both h-BN films are very smooth and clean, and the density of wrinkles is much lower than that of h-BN

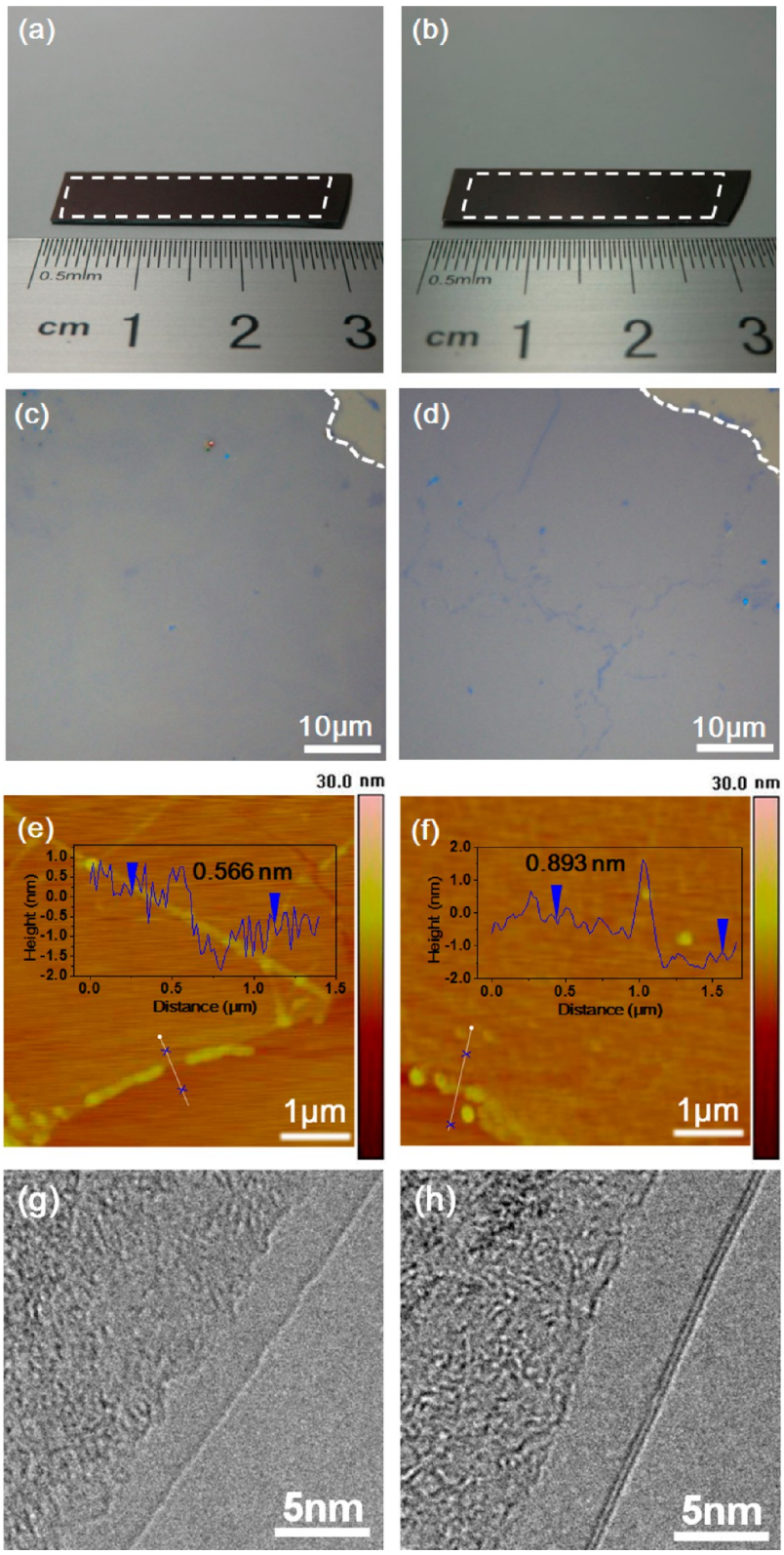

Figure 2. (a and b) Low-magnification optical, (c and d) high-magnification optical, (e and f) AFM, and (g and h) high-resolution TEM images of (a, c, e, g) monolayer and (b, d, f, h) bilayer h-BN films. The insets in (e) and (f) indicate the height profile along the white lines.

films grown on Cu foils,[7,24] indicating their high quality. In contrast, the few-layer h-BN films are very rough with many small islands on their surface (Figure S3).

We further analyzed the composition and structure of the h-BN films using X-ray photoelectron spectroscopy (XPS) and Raman spectroscopy. The B1s and N1s

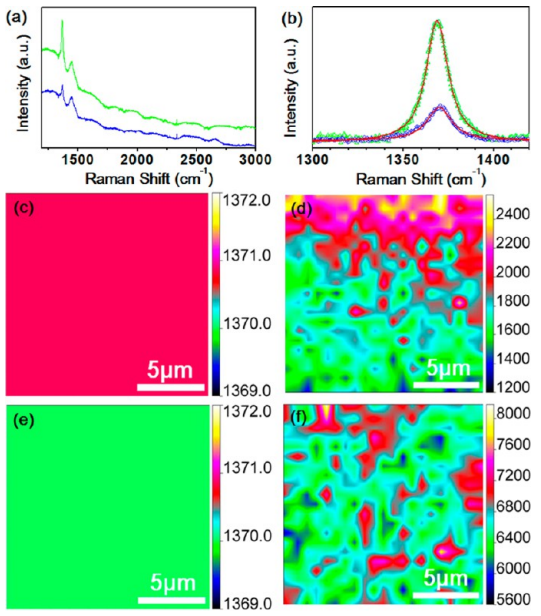

Figure 3. (a and b) Raman spectra of monolayer (blue curve and circles) and bilayer (green curve and circles) h-BN films. The red lines in (b) show the fitting to the Raman E_{2g} peak of h-BN. (c–f) Raman mappings of the (c and e) position and (d and f) intensity of the characteristic E_{2g} peaks of (c and d) monolayer and (e and f) bilayer h-BN films.

peaks of all the BN films are located at ~397 and 189 eV (Figure S4) respectively, similar to those reported for bulk h-BN. The derived atomic ratios of B to N for the monolayer and bilayer h-BN films are 1:1.03 and 1:1.07, respectively, very close to the 1:1 stoichiometry of h-BN. Moreover, they show a highly symmetric Raman peak at ~1370 cm^{-1} in the low frequency region (Figure 3a,b and S5), corresponding to the B–N vibrational mode (E_{2g}) within h-BN layers. As reported previously, the presence of decomposition byproducts of borazane in samples, such as c-BN, $B_xC_yN_z$ and BN soot, lead to asymmetric Raman peaks that can be deconvoluted into a 1370 cm^{-1} peak and some small peaks at lower frequencies.[12] Therefore, the symmetric characteristic Raman peak confirms the growth of high-purity BN films with a hexagonal structure. Moreover, this characteristic E_{2g} peak shifts to a lower frequency and its intensity and full width at half-maximum (fwhm) increase with increasing number of h-BN layers (Figure 3b and Figure S5). The E_{2g} peaks of the monolayer, bilayer and few-layer h-BN are located at ~1371, 1370, and 1368 cm^{-1}, and have fwhms of 15.6, 18.8, and 26.1 cm^{-1}, respectively. Considering the optical and AFM observations, we attributed the small fwhm of the monolayer h-BN to the micrometer-scale domain size. The upshifts and the smaller frequency difference of the E_{2g} peaks of our monolayer and bilayer h-BN with respect to those of monolayer and bilayer h-BN prepared by micromechanical cleavage are probably attributed to their different strain conditions, as discussed previously.[17] Figure 3c–f shows the mappings of the characteristic E_{2g} peak of the monolayer and bilayer h-BN films with an area of 15 × 15 μm^2. The position of E_{2g} peaks of both monolayer and bilayer h-BN is within 1 cm^{-1}, so the corresponding Raman mappings show the same color (Figure 3c,e). According to the statistical results shown in Table S3, the fwhm of the characteristic E_{2g} peaks of both monolayer and bilayer h-BN films is within 6 cm^{-1}, and about 86% and 88% areas show the same value, respectively. These results further confirm the high structural uniformity of our h-BN films.

The above results suggest that Pt is a good substrate for the controlled growth of high-quality monolayer and bilayer h-BN domains and continuous films by APCVD. In addition, after bubbling transfer of the h-BN the Pt substrates can be used for h-BN growth many times and no limit is currently observed. During the bubbling transfer process, a water reduction reaction ($2\ H_2O(l) + 2e^- \rightarrow H_2\ (g) + 2\ OH^-(aq)$) took place at the negatively charged cathode (Pt/h-BN/PMMA) to produce H_2.[28] Note that the Pt substrate is chemically inert to the electrolyte and is not involved in this chemical reaction. Therefore, similar to the transfer of graphene,[28] the bubbling delamination of h-BN does not destroy the Pt substrate and allows for repeated use of Pt for the CVD growth of h-BN without limit. In fact, all the Pt substrates have been reused for h-BN growth more than 200 times, and no obvious weight loss, structural change or thickness decrease of the substrate was observed (Figure S6a,b). This is completely different from the currently used growth substrate etching processes for the transfer of h-BN grown on Cu and Ni, and will effectively reduce environmental pollution caused by etching and also reduce the production cost of h-BN, which is especially important for the transfer of h-BN grown on noble metal substrates. When a Pt substrate was reused for the production of h-BN, no structural changes were observed in the product compared to the original, using the same growth conditions (Figure S6c,d).

The synthesis of h-BN with different thicknesses allows for studies on the effect of the number of layers on their various properties. As an example, we investigated the optical properties of h-BN by UV–visible absorption measurements. The UV–visible absorption spectra and the derived optical band gap (OBG) of the monolayer, bilayer and few-layer h-BN films are shown in Figure 4 and Figure S7. The OBG was derived using the equation:[32]

$$\alpha = C(E - E_g)^{1/2}/E$$

where α is the absorption coefficient, C is a constant, E is the photon energy of incident light, and E_g is the OBG. The absorption coefficient can be obtained by $\alpha = A/l$, where A is the optical absorption of the film measured by UV–vis spectrometry, and l is the average thickness of the film measured by AFM. Note that the plot of $(\alpha E)^2$ *versus* E gives a straight line, and therefore,

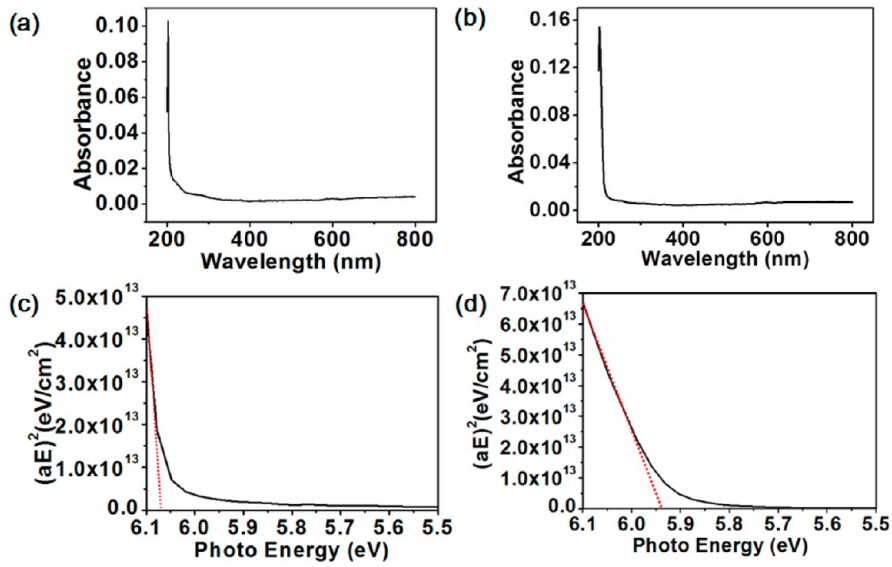

Figure 4. (a and b) UV−visible absorption spectra of (a) monolayer and (b) bilayer h-BN films transferred onto quartz substrates. (c and d) Optical band gap analysis from (a) and (b), respectively.

when $(\alpha E)^2 = 0$, the corresponding E value should be equal to E_g. It is interesting to find that the derived OBG increases with decreasing number of layers. The OBG is 6.07, 5.94, and 5.84 eV, for monolayer, bilayer, and few-layer h-BN, respectively. These values are larger than that (5.2−5.4 eV) of bulk h-BN.[33,34] The dependence of OBG on the number of layers indicates that interlayer interaction plays an important role in the electronic structure of h-BN, which can increase the dispersion of the electronic bands and consequently reduce the band gap.[33] The OBG obtained for monolayer h-BN is consistent with that (6.07 eV) of the monolayer grown on Cu[24] and close to that predicted by theoretical calculations (6.0 eV).[33]

The controlled growth of h-BN on Pt at different T_1 can be understood as follows. At low T_1 (70 °C), the decomposition of borazane is weak, and the product quantity is close to the balance point that needs for h-BN growth (at T_1 = 65 °C, no h-BN was formed on Pt). In this case, the h-BN growth follows a Frank van der Merwe model due to the adatom−surface (Pt) interaction,[35] leading to the formation of monolayer h-BN domains and films. Note that the two layers of a bilayer h-BN domain obtained in our experiments have the same shape and size (Figure 1d), which is similar to many other two-dimensional materials such as few-layer Bi_2Si_3, Bi_2Te_3, and MoS_2 obtained by van der Waals epitaxial growth.[36,37] Moreover, the number of layers of h-BN changes abruptly from monolayer to bilayer with T_1 without a transitional state (Figure S8). Therefore, we suggest that a bilayer nucleus forms when the quantity of borazane decomposition increases with increasing T_1 to 75 °C. After nucleation, the decomposition product of borazane tends to attach onto the edges of the two layers to form covalent bonds with increasing the reaction time because of the high reactivity of edges, leading to the lateral growth of the bilayer nuclei and the formation of bilayer domains and films. We believe that the growth of few-layer h-BN at a higher T_1 (80 °C) is similar to bilayers. The growth behavior of bilayer h-BN under our APCVD conditions is different from that of bilayer graphene reported in ref 38, where the adlayers and monolayer graphene grow by a similar self-limited surface adsorption process, and the adlayer growth proceeds by catalytic decomposition of methane (or CH_x, $x < 4$) trapped in a nanosized CVD chamber between the first layer and the substrate. Such difference is possibly due to the different interface interaction between metals and two-dimensional materials and the different growth conditions such as the chamber pressure. More experiments and theoretical work are required to fully understand this difference in the future. The appearance of additional layers on bilayer and few-layer h-BN films with extending the reaction time indicate that the growth of h-BN on Pt under our APCVD conditions is not self-limited, which is similar to the growth of monolayer h-BN under LPCVD.[24] In this case, the growth of h-BN follows a Stranski-Krastanov model.[35] More additional layers were formed on the surface of few-layer h-BN films compared to bilayer films because of the introduction of more decomposition product of borazane at higher T_1.

CONCLUSION

We reported the controlled growth of h-BN on Pt foils by low-cost APCVD with borazane as the precursor and its nondestructive transfer. Monolayer, bilayer and few-layer h-BN domains and large-area films were selectively obtained by simply changing the concentration of borazane introduced into the reaction system. Moreover, using the bubbling transfer method,

we have realized the repeated use of Pt for h-BN growth. The monolayer and bilayer h-BN obtained are very uniform with high quality and a smooth surface, while the few-layer h-BN shows a large surface roughness. In addition, we found that the optical band gap of h-BN increases with decreasing number of layers. The repeated growth of large-area, high-quality monolayer and bilayer h-BN films, together with the successful growth of graphene, opens up the possibility for creating various functional heterostructures for large-scale fabrication and integration of novel electronics.

EXPERIMENTAL SECTION

APCVD Growth of h-BN on Pt Foils. The synthesis of h-BN layers was carried out in a horizontal tube furnace (22 mm inner diameter tube) with a preposed heater using borazane as the precursor. The temperature of the reaction zone was fixed at 1000 °C during CVD growth. Pt foils (99.99%, 100 μm thick, 3 × 1 cm^2 in size) were first polished and put in the reaction zone before CVD growth. In a typical growth procedure, the borazane was placed in the preposed heater and heated to T_1 = 70−80 °C to produce borazane vapor, which was introduced by a 200 sccm Ar carrier gas flow and then mixed with an Ar/H_2 flow (Ar = 500 sccm, H_2 = 10 sccm) before reaching the reaction zone. After a certain growth time, the reaction was stopped by fast cooling. A filter was placed downstream of the preposed heater to hinder the introduction of nanosized BN particles produced by the vapor pyrolysis of borazane to the reaction zone.[24]

Bubbling Transfer. The electrochemical bubbling transfer process is similar to that reported previously for the transfer of graphene[28] and consists of the following steps: (a) Pt substrates with the grown h-BN were spin-coated with PMMA (4 wt % dissolved in ethyl lactate) at 2500 rpm for 1 min, and then cured at 180 °C for 10 min. (b) The PMMA/h-BN/Pt was dipped into a 1 M NaOH aqueous solution and used as the cathode of an electrolysis cell, with a Pt foil as anode. (c) The bubbling delamination of the PMMA/h-BN film was realized under a constant current of 0.1 A for ∼10 min. The corresponding electrolytic voltage was ∼3 V. (d) The PMMA/h-BN film was collected on target substrates, and the PMMA layer was then removed by hot acetone (40 °C) followed by drying in a N_2 flow.

Characterization. The morphology, structure and composition of h-BN layers were characterized using an optical microscope (Nikon Eclipse LV100), AFM (Veeco Dimension 3100, tapping mode), TEM (Tecnai F20, 200 kV) and XPS (ESCALAB250). The Raman spectra and mappings of h-BN layers were collected using a 532 nm laser with a Jobin Yvon LabRAM HR800, and the absorption spectra were measured by a UV−vis NIR spectrometer (Varian Cary 5000).

Conflict of Interest: The authors declare no competing financial interest.

Acknowledgment. This work was supported by National Science Foundation of China (Nos. 51172240, 51290273, 50921004 and 50972147), Ministry of Science and Technology of China (No. 2012AA030303) and Chinese Academy of Sciences (No. KGZD-EW-303-1).

Supporting Information Available: Schematic of the APCVD synthesis system used for h-BN growth; AFM image of bilayer h-BN domains transferred onto a SiO_2/Si substrate; optical, high-resolution TEM and AFM images of a few-layer h-BN film; XPS spectra of mono- and bilayer h-BN films on a SiO_2/Si substrate; Raman spectra of a few-layer h-BN film; Photos of a fresh and re-used Pt foil and optical images of repeated grown monolayer h-BN domains and film on a re-used Pt foil; UV−vis absorption spectrum of a few-layer h-BN film and OBG analysis; mono- and bilayer h-BN films obtained at the same growth conditions (T_1 = 72.5 °C); tables of h-BN structures produced in various conditions; analysis of the area coverage percentage of the additional layer spots on mono- and bilayer h-BN films; statistical analysis of the fwhm of the characteristic E_{2g} peaks of mono- and bilayer h-BN films. This material is available free of charge *via* the Internet at http://pubs.acs.org.

REFERENCES AND NOTES

1. Novoselov, K. S.; Geim, A. K.; Morozov, S. V.; Jiang, D.; Zhang, Y.; Dubonos, S. V.; Grigorieva, I. V.; Firsov, A. A. Electric Field Effect in Atomically Thin Carbon Films. *Science* **2004**, *306*, 666–669.
2. Geim, A. K.; Novoselov, K. S. The Rise of Graphene. *Nat. Mater.* **2007**, *6*, 183–191.
3. Geim, A. K. Graphene: Status and Prospects. *Science* **2009**, *324*, 1530–1534.
4. Kubota, Y.; Watanabe, K.; Tsuda, O.; Taniguchi, T. Deep Ultraviolet Light-Emitting Hexagonal Boron Nitride Synthesized at Atmospheric Pressure. *Science* **2007**, *317*, 932–934.
5. Sugino, T.; Tai, T. Dielectric Constant of Boron Nitride Films Synthesized by Plasma-Assisted Chemical Vapor Deposition. *Jpn. J. Appl Phys., Part 2* **2000**, *39*, L1101–L1104.
6. Ci, L.; Song, L.; Jin, C.; Jariwala, D.; Wu, D.; Li, Y.; Srivastava, A.; Wang, Z. F.; Storr, K.; Balicas, L.; Liu, F.; *et al.* Atomic Layers of Hybridized Boron Nitride and Graphene Domains. *Nat. Mater.* **2010**, *9*, 430–435.
7. Song, L.; Ci, L.; Lu, H.; Sorokin, P. B.; Jin, C.; Ni, J.; Kvashnin, A. G.; Kvashnin, D. G.; Lou, J.; Yakobson, B. I.; *et al.* Large Scale Growth and Characterization of Atomic Hexagonal Boron Nitride Layers. *Nano Lett.* **2010**, *10*, 3209–3215.
8. Chen, Y.; Zou, J.; Campbell, S. J.; Le Caer, G. Boron Nitride Nanotubes: Pronounced Resistance to Oxidation. *Appl. Phys. Lett.* **2004**, *84*, 2430–2432.
9. Watanabe, K.; Taniguchi, T.; Kanda, H. Direct-Bandgap Properties and Evidence for Ultraviolet Lasing of Hexagonal Boron Nitride Single Crystal. *Nat. Mater.* **2004**, *3*, 404–409.
10. Castro Neto, A. H.; Peres, N. M. R.; Novoselov, K. S.; Geim, A. K. The Electronic Properties of Graphene. *Rev. Mod. Phys.* **2009**, *81*, 109–162.
11. Dean, C. R.; Young, A. F.; Meric, I.; Lee, C.; Wang, L.; Sorgenfrei, S.; Watanabe, K.; Taniguchi, T.; Kim, P.; Shepard, K. L.; *et al.* Boron Nitride Substrates for High-Quality Graphene Electronics. *Nat. Nanotechnol.* **2010**, *5*, 722–726.
12. Lee, K. H.; Shin, H. J.; Lee, J.; Lee, I. Y.; Kim, G. H.; Choi, J. Y.; Kim, S. W. Large-Scale Synthesis of High-Quality Hexagonal Boron Nitride Nanosheets for Large-Area Graphene Electronics. *Nano Lett.* **2012**, *12*, 714–718.
13. Britnell, L.; Gorbachev, R. V.; Jalil, R.; Belle, B. D.; Schedin, F.; Mishchenko, A.; Georgiou, T.; Katsnelson, M. I.; Eaves, L.; Morozov, S. V.; *et al.* Field-Effect Tunneling Transistor Based on Vertical Graphene Heterostructures. *Science* **2012**, *335*, 947–950.
14. Britnell, L.; Gorbachev, R. V.; Jalil, R.; Belle, B. D.; Schedin, F.; Katsnelson, M. I.; Eaves, L.; Morozov, S. V.; Mayorov, A. S.; Peres, N. M. R.; *et al.* Electron Tunneling through Ultrathin Boron Nitride Crystalline Barriers. *Nano Lett.* **2012**, *12*, 1707–1710.
15. Novoselov, K. S.; Jiang, D.; Schedin, F.; Booth, T. J.; Khotkevich, V. V.; Morozov, S. V.; Geim, A. K. Two-Dimensional Atomic Crystals. *Proc. Natl. Acad. Sci. U.S.A.* **2005**, *102*, 10451–10453.
16. Pacilé, D.; Meyer, J. C.; Girit, C. O.; Zettl, A. The Two-Dimensional Phase of Boron Nitride: Few-Atomic-Layer Sheets and Suspended Membranes. *Appl. Phys. Lett.* **2008**, 92.
17. Gorbachev, R. V.; Riaz, I.; Nair, R. R.; Jalil, R.; Britnell, L.; Belle, B. D.; Hill, E. W.; Novoselov, K. S.; Watanabe, K.; Taniguchi, T.; *et al.* Hunting for Monolayer Boron Nitride: Optical and Raman Signatures. *Small* **2011**, *7*, 465–468.

18. Coleman, J. N.; Lotya, M.; O'Neill, A.; Bergin, S. D.; King, P. J.; Khan, U.; Young, K.; Gaucher, A.; De, S.; Smith, R. J.; Shvets, I. V.; *et al.* Two-Dimensional Nanosheets Produced by Liquid Exfoliation of Layered Materials. *Science* **2011**, *331*, 568–571.
19. Shi, Y.; Hamsen, C.; Jia, X.; Kim, K. K.; Reina, A.; Hofmann, M.; Hsu, A. L.; Zhang, K.; Li, H.; Juang, Z. Y.; *et al.* Synthesis of Few-Layer Hexagonal Boron Nitride Thin Film by Chemical Vapor Deposition. *Nano Lett.* **2010**, *10*, 4134–4139.
20. Corso, M.; Auwarter, W.; Muntwiler, M.; Tamai, A.; Greber, T.; Osterwalder, J. Boron Nitride Nanomesh. *Science* **2004**, *303*, 217–220.
21. Sutter, P.; Lahiri, J.; Albrecht, P.; Sutter, E. Chemical Vapor Deposition and Etching of High-Quality Monolayer Hexagonal Boron Nitride Films. *ACS Nano* **2011**, *5*, 7303–7309.
22. Nagashima, A.; Tejima, N.; Gamou, Y.; Kawai, T.; Oshima, C. Electronic Dispersion-Relations of Monolayer Hexagonal Boron-Nitride Formed on the Ni(111) Surface. *Phys. Rev. B* **1995**, *51*, 4606–4613.
23. Auwarter, W.; Suter, H. U.; Sachdev, H.; Greber, T. Synthesis of One Monolayer of Hexagonal Boron Nitride on Ni(111) from B-Trichloroborazine $(ClBNH)_3$. *Chem. Mater.* **2004**, *16*, 343–345.
24. Kim, K. K.; Hsu, A.; Jia, X.; Kim, S. M.; Shi, Y.; Hofmann, M.; Nezich, D.; Rodriguez-Nieva, J. F.; Dresselhaus, M.; Palacios, T.; *et al.* Synthesis of Monolayer Hexagonal Boron Nitride on Cu Foil Using Chemical Vapor Deposition. *Nano Lett.* **2012**, *12*, 161–166.
25. Joshi, S.; Ecija, D.; Koitz, R.; Iannuzzi, M.; Seitsonen, A. P.; Hutter, J.; Sachdev, H.; Vijayaraghavan, S.; Bischoff, F.; Seufert, K.; *et al.* Boron Nitride on Cu(111): An Electronically Corrugated Monolayer. *Nano Lett.* **2012**, *12*, 5821–5828.
26. Preobrajenski, A. B.; Vinogradov, A. S.; Ng, M. L.; Cavar, E.; Westerstrom, R.; Mikkelsen, A.; Lundgren, E.; Martensson, N. Influence of Chemical Interaction at the Lattice-Mismatched h-BN/Rh(111) and h-BN/Pt(111) Interfaces on the Overlayer Morphology. *Phys. Rev. B* **2007**, *75*.
27. Ismach, A.; Chou, H.; Ferrer, D. A.; Wu, Y. P.; McDonnell, S.; Floresca, H. C.; Covacevich, A.; Pope, C.; Piner, R.; Kim, M. J.; *et al.* Toward the Controlled Synthesis of Hexagonal Boron Nitride Films. *ACS Nano* **2012**, *6*, 6378–6385.
28. Gao, L.; Ren, W.; Xu, H.; Jin, L.; Wang, Z.; Ma, T.; Ma, L. P.; Zhang, Z.; Fu, Q.; Peng, L. M.; *et al.* Repeated Growth and Bubbling Transfer of Graphene with Millimetre-Size Single-Crystal Grains Using Platinum. *Nat. Commun.* **2012**, *3*, 699.
29. Guo, N.; Wei, J. Q.; Fan, L. L.; Jia, Y.; Liang, D. Y.; Zhu, H. W.; Wang, K. L.; Wu, D. H. Controllable Growth of Triangular Hexagonal Boron Nitride Domains on Copper Foils by an Improved Low-Pressure Chemical Vapor Deposition Method. *Nanotechnology* **2012**, 23.
30. Laskowski, R.; Blaha, P. *Ab Initio* Study of *h*-BN Nanomeshes on Ru(001), Rh(111), and Pt(111). *Phys. Rev. B* **2010**, 81.
31. Vlassiouk, I.; Regmi, M.; Fulvio, P.; Dai, S.; Datskos, P.; Eres, G.; Smirnov, S. Role of Hydrogen in Chemical Vapor Deposition Growth of Large Single-Crystal Graphene. *ACS Nano* **2011**, *5*, 6069–6076.
32. Yuzuriha, T. H.; Hess, D. W. Structural and Optical-Properties of Plasma-Deposited Boron-Nitride Films. *Thin Solid Films* **1986**, *140*, 199–207.
33. Blase, X.; Rubio, A.; Louie, S. G.; Cohen, M. L. Quasiparticle Band Structure of Bulk Hexagonal Boron Nitride and Related Systems. *Phys. Rev. B* **1995**, *51*, 6868–6875.
34. Hoffman, D. M.; Doll, G. L.; Eklund, P. C. Optical-Properties of Pyrolytic Boron-Nitride in the Energy-Range 0.05−10 eV. *Phys. Rev. B* **1984**, *30*, 6051–6056.
35. Pimpinelli, A.; Villain, J. *Introduction to Surface and Thin Films Processes*; Cambridge University Press: New York, 1998.
36. Kong, D.; Dang, W.; Cha, J. J.; Li, H.; Meister, S.; Peng, H.; Liu, Z.; Cui, Y. Few-Layer Nanoplates of Bi_2Se_3 and Bi_2Te_3 with Highly Tunable Chemical Potential. *Nano Lett.* **2010**, *10*, 2245–2250.
37. Shi, Y. M.; Zhou, W.; Lu, A. Y.; Fang, W. J.; Lee, Y. H.; Hsu, A. L.; Kim, S. M.; Kim, K. K.; Yang, H. Y.; Li, L. J.; *et al.* van der Waals Epitaxy of MoS_2 Layers Using Graphene as Growth Templates. *Nano Lett.* **2012**, *12*, 2784–2791.
38. Li, Q.; Chou, H.; Zhong, J. H.; Liu, J. Y.; Dolocan, A.; Zhang, J.; Zhou, Y.; Ruoff, R. S.; Chen, S.; Cai, W. Growth of Adlayer Graphene on Cu Studied by Carbon Isotope Labeling. *Nano Lett.* **2013**, *13*, 486–490.